Paper No.
11071

NACE INTERNATIONAL CORROSION 2018 Conference & Expo

Corrosion Behavior of Naphthenic Acids Isolated from Vacuum Gas Oil Fractions

Yathish Kurapati, Winston Robbins, Gheorghe Bota, David Young
Institute for Corrosion and Multiphase Technology
Department of Chemical & Biomolecular Engineering, Ohio University
342 West State Street, Athens, OH 45701

ABSTRACT

Opportunity crudes frequently have increased acidity, making high temperature naphthenic acid (NAP) corrosion a key concern for their processing in refineries. Lab corrosion rates are hard to interpret due to either variable composition of crude fractions or the use of commercially available model carboxylic acids that may be unrepresentative of NAP species present in vacuum gas oils (VGO). Here, the corrosion behavior of native naphthenic acids in two VGO fractions are compared with white oil solutions of the acids isolated from them by solid phase extraction (SPE). Corrosion tests are conducted per the in-house "pretreatment-challenge" protocol on carbon steel and 5Cr steel samples. Corrosion rates for isolated acid solutions in mineral oil are lower than those for the corresponding VGO. Corrosion product scales formed by the isolated acids are more resistant than VGO to a high severity acid-only challenge. Characterization of corrosion product scales by cross-section electron microscopy techniques confirm that the isolated acids generate dense oxide-rich layers under thin iron sulfide (FeS) layers, in contrast to the oxide layers observed under thicker sulfide layers for the VGO. The resistance of the oxide layers to the acid challenge is consistent with previously reported formation of nano-particulate magnetite (Fe_3O_4).

Key words: *Naphthenic acids, solid phase extraction, magnetite, NAP extraction, sulfidation*

INTRODUCTION

Crude oil price fluctuations and the need to improve refinery margins have driven refiners towards utilizing "opportunity crudes," despite the challenges frequently associated with their processing. Most opportunity crudes have increased acidity and reactive sulfur compounds, making high temperature (~220–400°C) sulfidation-naphthenic acid (SNAP) corrosion a key concern for process and corrosion engineers.[1,2] Naphthenic acids (NAP) are naturally occurring carboxylic acids in crude oil that are typically measured by Total Acid Number (TAN – mg of KOH required to neutralize acid in one gram of oil). Crude oil contains a wide variety of sulfur compounds, some reactive and some not – reactive sulfur compounds thermally decompose to form hydrogen sulfide (H_2S) that reacts with the steel surface. It is widely accepted that the corrosion from naphthenic acids and sulfur compounds can be represented by the following reactions: [3, 4]

$$Fe + 2RCOOH \rightarrow Fe(RCOO)_2 + H_2 \quad (1)$$

$$Fe + H_2S \rightarrow FeS + H_2 \quad (2)$$

$$Fe(RCOO)_2 + H_2S \leftrightarrow FeS + 2RCOOH \quad (3)$$

Equation (1) and Equation (2) represent oxidation of metallic iron by naphthenic acids (RCOOH) and hydrogen sulfide (H_2S - a surrogate for, and product of, reactive sulfur compounds), respectively. Iron naphthenates ($Fe(RCOO)_2$) formed in NAP corrosion are oil soluble and are considered to be depleted by the flow. Iron sulfide (FeS) formed in sulfidation is insoluble in oil and grows as a scale on the metal surface.[4-7] Secondary reactions, Equation (3), that may occur in the bulk liquid are proposed to affect corrosion indirectly by regenerating corrosive species.

SNAP corrosion is a complex phenomenon that is affected by a wide range of parameters including temperature, flow, type of sulfur species, NAP species, TAN, sulfur (wt. %), and metallurgy. Laboratory research aimed at determining the role of NAP in corrosion is commonly performed with real crude fractions, commercially available NAP acid mixtures, or model carboxylic acids. Each of these approaches has inherent limitations. Crude oil distillates' matrix interactions, especially those due to sulfur, complicate interpretation of corrosion by NAP acids.[2-4] Even if isolated from petroleum sources, commercial NAP acids may not be representative of the boiling range (molecular weight) of acids found in vacuum gas oils.[2,8] The majority of naphthenic acids from commercial sources boil at temperatures lower than those of vacuum gas oils, where SNAP is of greatest interest.[8] Carboxylic acids, available as model compounds for laboratory corrosion tests, generally lack the structural characteristics of naphthenic acids: short -CH_2COOH side chains attached to 1-4 saturated rings.[9-11] Many of these characteristics of NAP were identified after their isolation for analytical evaluation. The separation techniques, however, can be adapted for isolation of sufficient NAP acids for corrosion testing at the laboratory scale.[8,11] In one case, more corrosion was observed for lower boiling range acids (at 250ºC actual temperature).[8] At these low temperatures, minimal scale formation was observed by plane-view scanning electron microscopy (SEM). However, weight loss measurement and SEM cross-section analyses have shown that scale formation and composition have a significant impact on VGO corrosion rates at temperatures >300ºC.[6,7,12-14]

NAP acids have been isolated from two HVGOs with different corrosion and scale behaviors in order to assess the role of the acids, *i.e.*, to decouple the effect of NAP acids from the HVGO matrix relating to corrosion. The isolation of these acids from a HVGO matrix was achieved using solid phase extraction with aminopropyl silica (APS) and the evaluation of the "isolated NAP acids" with respect to corrosion in an inert mineral oil (spiked to native TAN) as per the "Pretreatment – Challenge" protocol developed at the Institute for Corrosion and Multiphase Technology (ICMT) at Ohio University.[6,7]

STAGE 1 – NAP ACID ISOLATION

The bulk quantities of NAP acids needed for corrosion testing were isolated from the HVGO fractions by an SPE procedure using an amine-functionalized silica – aminopropyl silica (APS) that has been used previously on an analytical scale.[15] In this procedure, NAP acids present in HVGO are adsorbed onto the APS while the bulk of the oil is removed with solvents and then the NAP acids are displaced with excess acetic acid in toluene, as detailed below (Figure 1).

Equal volumes of a weighed HVGO sample and toluene are combined in a flask to reduce viscosity. A three-fold molar excess of APS (Sigma-Aldrich, St. Louis MO), based on sample TAN, is added to the solution and stirred overnight for 12 hours. The APS slurry is then poured through a porous cellulose Soxhlet extraction thimble (GE Whatman, UK) so that the APS with adsorbed NAP acids is retained in the thimble and the acid-depleted oil is collected in a beaker. The thimble is then loaded into a Soxhlet extractor with toluene in the boiling flask to extract residual oil. After the residual oil/toluene extract solution is removed, an azeotropic solution of acetic acid: toluene (70:30) is placed in the boiling flask. NAP acids are extracted by mass action into the boiling flask solution by the azeotrope so that the APS remaining in the thimble has acetic acid adsorbed on its active sites. The bulk of the solvent mixture is removed from the NAP acids by rotary evaporation (WG-EV311 rotary evaporator - Wilmad-LabGlass, Vineland, NJ). The traces of acetic acid remaining in the residual NAP acid-toluene solution are

eliminated by multiple washes with distilled water in a separatory funnel. Acetic acid, being soluble in water, goes into the aqueous phase, and NAP acids remain in the toluene phase. The water phase is discarded, and the toluene phase containing NAP acids is retained. The NAP acid extract is recovered by removal of toluene with rotary evaporation at a higher temperature. The toluene solutions filtered through the Soxhlet thimble are designated “acid depleted oil” and toluene Soxhlet extracts are identified as “residual oil.” Each is retained for further use.

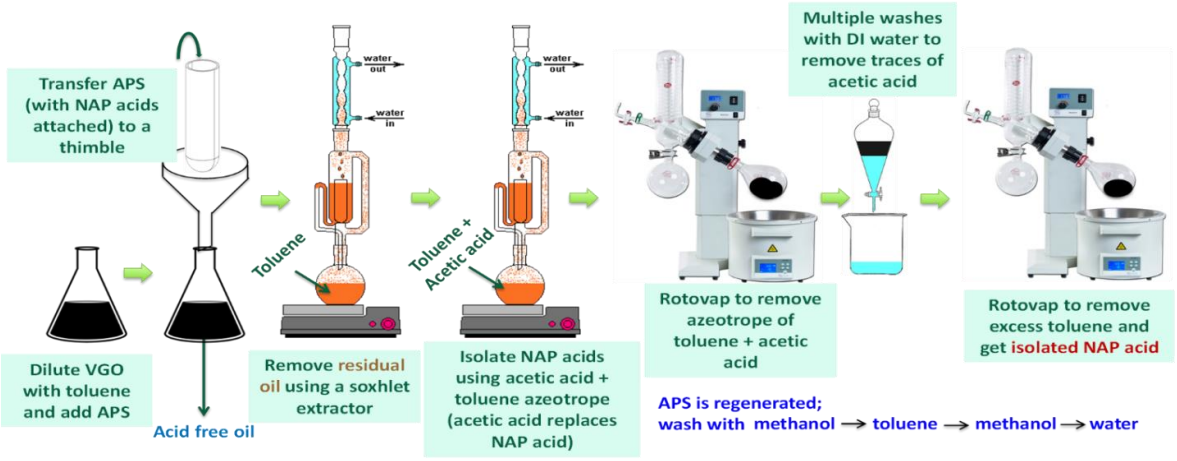

Figure 1: Schematic representation of the sequence of steps employed to isolate NAP acids.

The amount of HVGO used for NAP acid extraction is limited by the size of the Soxhlet extraction apparatus. With the existing apparatus, only 500g - 550g of HVGO can be processed. Therefore, the acid isolation procedure had to be performed in two batches to obtain enough NAP acid extract to conduct the corrosion tests. The efficiency of the process is monitored by measuring total acid number (TAN) in the oils (after toluene stripping) at different stages of the isolation procedure by potentiometric titration as per ASTM D664 [15, 16] (Table 1). NAP acid extracts obtained from different batches are mixed together and diluted in mineral oil such that final TAN of the solution is the same as their respective native HVGO fraction. Small amounts of sulfur seen in NAP acid extracts is attributed to the presence of sulfur as a component part of the molecular structure of particular naphthenic acids.

Extraction yield (%) in Table 1 is calculated as per Equation (4).

$$Extraction\ yield\ (\%) = \frac{W_2 * TAN_{extract}}{W_1 * TAN_{initial}} * 100 \quad (4)$$

Where,

W_1= Initial weight of the HVGO fraction [g]
W_2= Final weight of the NAP acid extract [g]
$TAN_{initial}$= TAN of native HVGO fraction
$TAN_{extract}$= TAN of final NAP acid extract

The isolated acid extracts were diluted in an acid/S-free heavy mineral oil to prepare test solutions with NAP acid concentrations close to that of the native HVGO. The TAN of these test oils were determined by TAN titration. The concentration of S was estimated from that of HVGO’s and the dilution factor (previous studies have shown that concentration of S in isolated acids is close to that of their source oil [8,11]; this may be due to the nature of their biogeochemical origin[17]). The data show that the TANs of the “Acid Solutions” are close to their parent HVGO, but the sulfur concentrations have been reduced approximately 20 fold; *i.e.*, molar ratio of S/TAN has been reduced 20 fold. In previous publications, it has been noted that the S/TAN ratio affects the nature of the scales formed and that scales from HVGO are more complex than those from model acids.[7, 18]

Table 1
TAN (mg KOH/g oil) Measured in Oils after Solvent Stripping at Different Stages of NAP Acid Extraction

	HVGO-A		*HVGO-B*	
SAMPLE	**Batch 1**	**Batch 2**	**Batch 1**	**Batch 2**
Native fraction	5.93	5.93	4.43	4.43
Acid depleted oil	0.241	0.32	0.33	0.29
Residual oil	1.14	1.29	0.91	0.54
Final NAP acid extract	144.5	131.2	96.1	111.5
Extraction yield (%)	86.9	86	88.4	88.6

Table 2
TAN and Estimated Total Sulfur Content of the "HVGO" and its "NAP Acid Extract Solution in Mineral Oil"

	HVGO-A	*Acids A Solution*	*HVGO-B*	*Acids B Solution*
TAN (mg KOH/g oil)	5.93	5.85	4.43	4.49
Sulfur (wt. %)	0.87	0.04	3.65	0.15
S/TAN	0.15	0.007	0.83	0.031
Mole ratio S/acid	2.56	0.12	19.4	0.50

STAGE 2 – EXPERIMENTAL DETAILS

Corrosion characteristics of isolated naphthenic acids are evaluated per ICMT's in-house "Pretreatment – Challenge" protocol.[9, 16] This specific experimental protocol involves two corrosion tests. In the first test, the steel samples are pretreated with test fluids containing corrosive species to determine the corrosion rates and corrosion scale characteristics. In the second test, samples are pretreated in the same manner and then are challenged in a more aggressive environment to determine the protectiveness of corrosion product scale formed during pretreatment.

Equipment Description

Autoclave

A static 1L autoclave (AUT) made of Alloy C-276 (Parr Instruments, IL) is used for pretreatment. A schematic of the autoclave is shown in Figure 2. The autoclave has a magnetic stirrer coupled to an impeller which homogenizes the experimental fluid during the test. Two valves located on the autoclave head are used to purge the AUT headspace with nitrogen before and after the test, for deoxygenation and for evacuation of generated toxic vapors, respectively. Test samples are placed on specific sample holders (shown in Figure 2) and then immersed in the experimental fluid in the AUT. Temperature of the test fluid is monitored/controlled during tests through a thermocouple inserted into a thermowell. Pressure in the autoclave is monitored with the attached gauge.

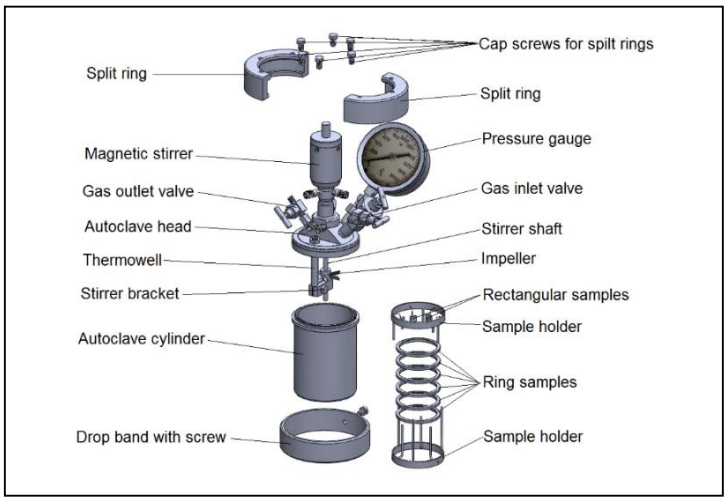

Figure 2: Static autoclave (AUT) set-up used for "pretreatment."

High Velocity Rig (HVR)

"Challenge" tests are conducted in a high velocity rig (HVR) that is designed for use at high temperature, shear stress and velocity conditions. The HVR is a flow through system where the test fluids are preheated and pumped continuously through the autoclave containing the metal samples. Only "ring" shaped samples can be handled in the HVR. The "ring" samples are mounted on a rotating cylinder which is located inside the HVR autoclave. During the test, the cylinder rotates at 2000 rpm that corresponds to peripheral velocity of 8.5 m/s. Thus, it becomes possible to expose samples to high temperature and high velocity simultaneously in a corrosive environment during the HVR test. The HVR heating (AUT, feeding lines), temperature control, oil flow (pump), sample rotation (AUT), and test duration are controlled by a PC with specific software. Some details of the HVR (rotating cylinder, cross-sectional view) are shown in Figure 3. More detailed description and the schematic can be obtained from our earlier work by Bota, *et al.*[7]

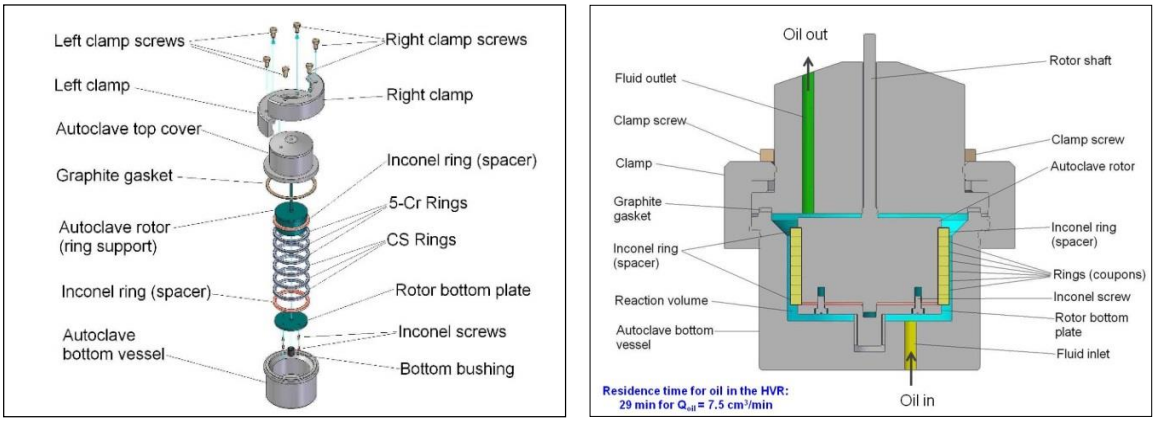

Figure 3: (a) Schematic representation of rotating cylinder, samples and autoclave in HVR (b) Cross sectional view of HVR.

Test Solutions

NAP acid extracts obtained from SPE are mixed in highly refined mineral oil and spiked to their respective native TAN. Native HVGO fractions and their NAP acid extract mixtures in mineral oil are used

in “pretreatment.” A commercial mixture of naphthenic acids (TCI America) extracted from petroleum was dissolved in the same mineral oil to prepare a “corrosive TAN 3.5” solution that is used in “challenge” tests – this is referred to as “TAN 3.5 Challenge solution.” The characteristics of the test fluids and experimental conditions for pretreatment are outlined in Table 3. For challenge, all pretreatment tests in Table 3 are repeated and then challenged in HVR with ‘‘TAN 3.5 Challenge solution.’’ Samples generated in “pretreatment” are used to calculate pretreatment corrosion rate and, hence, fresh samples need to be pretreated before they are challenged in HVR. Procedures to calculate corrosion rates are expanded upon in a later section.

Test Materials

Corrosion tests were performed on two materials - A106 carbon steel (CS) and F5 A182 steel (5Cr steel). These materials are chosen as they are most commonly used in refineries. Test samples of two different geometries are used - ring samples (OD = 81.76 mm, ID = 70.43 mm and width, H = 5 mm) and rectangular samples (CS samples of dimensions 19.2 mm x 12.8 mm x 3.2 mm and 5Cr steel samples of dimensions 17.7 mm x 11.1 mm x 3.2 mm). Ring samples are used to calculate corrosion rates while rectangular samples are used for characterization of pretreatment corrosion product scales (TEM/SEM/EDS). Before experiments, each sample was polished with 400 and 600-grit silicon carbide paper (SiC), in succession. Isopropanol was used to flush samples during polishing to prevent oxidation and overheating. After polishing, samples were wiped with a paper towel, rinsed with toluene and acetone, and dried under nitrogen flow. Initial weights of polished clean samples were measured with an analytical balance capable of measuring accurately up to 0.1 mg.

After each experiment, samples were rinsed with toluene and acetone, gently rubbed with a soft plastic brush, treated with “Clarke” solution (ASTM G1-03) and reweighed. Based on the weight difference of samples before and after the experiment and the exposed surface area, the corrosion rate was calculated.

Test Procedures

Pretreatment in Autoclave

In “pretreatment”, the static autoclave is filled with test fluid up to 60% of its volume – providing enough head space to accommodate vapors generated during testing as well as liquid expansion. A sample holder containing ring samples and rectangular samples is placed in the autoclave vessel such that samples are fully immersed in the test fluid. The autoclave head is clamped to the vessel, and the autoclave head space is flushed with nitrogen for a few minutes (typically ~10 minutes) to deoxygenate the system. Temperature of the test fluid is raised to 650°F (343°C) and is maintained for 24 hours. During the entire test, the magnetic stirrer is switched on and the test fluid is constantly agitated. After 24 hours, heating is turned off and the system is allowed to undergo cooling. After reaching room temperature, the head space is flushed with nitrogen to remove toxic vapors generated during the test and samples are processed for weight loss analysis.

Challenge in High Velocity Rig

In the “pretreatment-challenge” test, samples are initially pretreated in the autoclave under the same conditions as described above. After reaching room temperature, all ring samples are transferred onto a rotating cylinder in the HVR. “TAN 3.5 Challenge solution” of TCI acids in mineral oil is preheated to 650°F (343°C) and flows through the HVR autoclave at a rate of 7.5 cm^3/min throughout the test. The pretreated samples are exposed to “TAN 3.5 Challenge solution” for 24 hours, after which heating is turned off. The system is allowed to cool down and the samples are removed for further analysis. One carbon steel and one 5Cr steel sample is stored in mineral oil for SEM analysis, while the other samples are processed immediately for weight-loss analysis.
In addition to challenging pretreated samples, as a benchmark experiment, freshly-polished samples without any pretreatment were installed in the HVR and corroded by the “TAN 3.5 Challenge solution” at

the same conditions as for the other tests. The corrosion rate obtained in this experiment is referred to as "pure TAN 3.5 corrosion rate." The pretreated samples are expected to have lower challenge corrosion rates than "pure TAN 3.5 corrosion rate" due to formation of protective corrosion product scales during "pretreatment."

Table 3
Experimental Matrix for "Pretreatment" in Autoclave

Test No.	Pretreatment in Autoclave				
	Test fluid	Sulfur (Wt. %)	TAN (mg KOH/g)	Time (h)	Temp. (°F)
1	HVGO-A	0.87	5.93	24	650
2	HVGO-B	3.65	4.43	24	650
3	Acids A in mineral oil	0.04	5.85	24	650
4	Acids B in mineral oil	0.15	4.49	24	650

Corrosion Rate Evaluation

Corrosion rates of samples are assessed based on their weight loss during the experiment. "Pretreatment" and "Challenge" corrosion rates are calculated using Equation (5) and Equation (6), respectively. For every test, three carbon steel samples and three 5Cr steel samples are used, and the reported corrosion rate is the average value of those obtained for these three samples.

$$CR_{Pretreatment} = \frac{IW - FW}{\rho_{steel} * A_{S,Pretreatment} * t_{Pretreatment}} * 10 * 24 * 365 \quad (5)$$

$$CR_{Challenge} = \frac{IW - FW - WL_{Pretreatment}}{\rho_{steel} * A_{S,Challenge} * t_{Challenge}} * 10 * 24 * 365 \quad (6)$$

Where,

$CR_{Pretreatment}$ – Pretreatment corrosion rate, [mm/y]
IW – Initial weight of freshly polished sample, [g]
FW – Final weight of steel sample after treating with Clarke solution, [g]
ρ_{steel} – Density of steel sample, [g/cm^3]
$A_{S,Pretreatment}$ – Area of sample exposed to test fluid during pretreatment, [cm^2]
$t_{Pretreatment}$ – Duration of pretreatment, [h]
$CR_{Challenge}$ – Corrosion occurred during the challenge step only, [mm/y]
$WL_{Pretreatment}$ – Weight loss of sample in pretreatment step, [g]
$A_{S,Challenge}$ – Area of sample exposed to test fluid during challenge, [cm^2]
$t_{Challenge}$ – Duration of challenge test in HVR, [h]

Microscopic Analysis

Cross-sections of all samples were examined by a scanning electron microscope (SEM), equipped with a silicon drift detector for energy dispersive spectroscopy (EDS) compositional analysis across the layers. Some of the pretreated samples were analyzed using a Transmission Electron Microscope (FEI Tecnai F30 TEM), as it is more suitable to characterize thin scales up to resolution as high as 0.3 nm. Phase analysis of inner scale was carried out using Precession Electron Diffraction (PED), a feature available in

TEM, as traditional X-ray diffraction cannot detect phases for inner corrosion product scales. TEM samples were extracted by a focused ion beam (FIB).

EXPERIMENTAL RESULTS

HVGO-A vs. "Acids A" (NAP Acids Extracted from HVGO-A in Mineral Oil)

Corrosion rates determined for CS and 5Cr steel during pretreatment and challenge tests are shown in Figure 4. During pretreatment, "Acids A" are as corrosive as "HVGO-A" on carbon steel, but less corrosive on 5Cr steel. However, in the "challenge" test, both CS and 5Cr samples pretreated with "Acids A" resist the TAN 3.5 acid challenge. This indicates that the corrosion product scales formed by "Acids A" are very protective, *i.e.*, they are resistant to naphthenic acid attack. Thus, although "HVGO-A" itself shows some resistance to naphthenic acid corrosion, isolation of naphthenic acids enhances the resistance. To better understand the reason for this enhanced resistance of the corrosion product scale, samples were subjected to an extensive analysis of the corrosion scale on pretreated samples using SEM/EDS and FIB-TEM/PED techniques.

SEM analyses showed that the films from "Acids A pretreatment" were very thin, so the cross-sections of CS and 5Cr samples were analyzed by TEM (Figure 5). The inner and outer layers are continuous, of similar < 1µm thickness, and appear to differ in density and morphology in the TEM images. Composition analysis using EDS elemental mapping showed that the two layers are dissimilar, *i.e.*, the outer layer predominantly shows the presence of sulfur and iron, while the inner layer is composed of iron and oxygen. In the case of 5Cr samples, Cr was also seen in the inner layer. EDS line scanning (Figure 5) across the scales further strengthens the observation that the two layers are different in composition. In order to gain further knowledge about the different phases present in the corrosion products, phase analysis was carried out using Precession Electron Diffraction (PED).

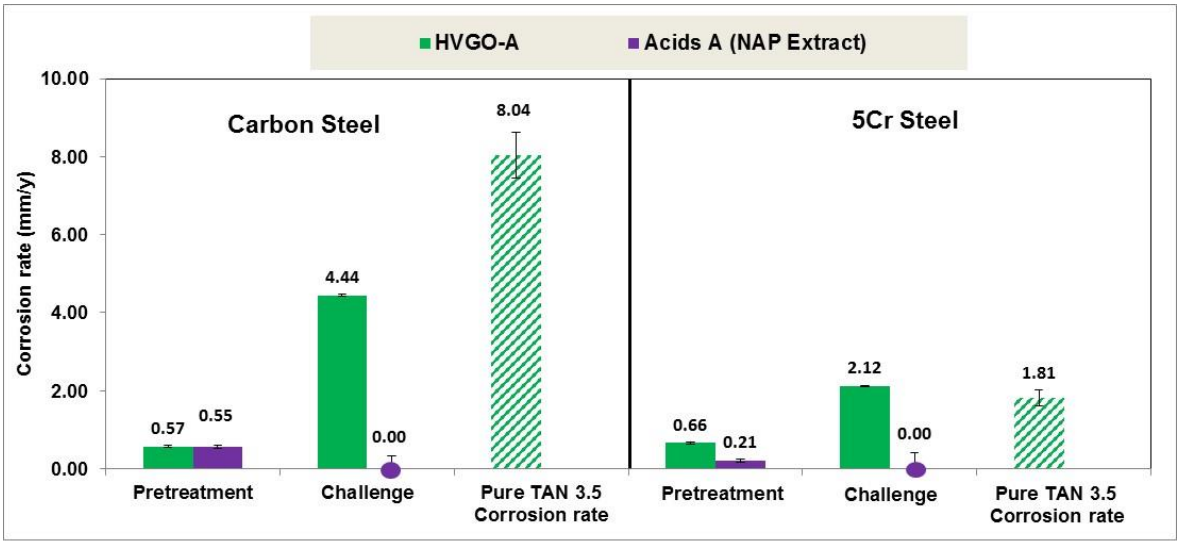

Figure 4: Comparison of pretreatment and challenge corrosion rates for CS and 5Cr steel samples that are pretreated using HVGO-A and its NAP Acid extract (Acids A) and challenged with 'TAN 3.5 challenge' solution.

Precession electron diffraction (PED) is an add-on to the TEM and, hence, is done after obtaining the TEM images at high resolution. PED spot patterns are collected sequentially with a dedicated external camera while the primary electron beam scans the sample area (typically a few square micrometers chosen from the area of interest on the TEM image) and simultaneously precessed around the optical

axis of the microscope. During this scanning and precessing of the primary electron beam, thousands of PED spot patterns are recorded and stored in the computer's memory. In order to proceed with crystal orientation and phase identification of each experimental PED spot pattern, thousands of simulated spot patterns (so-called templates) are utilized for each crystallographic phase in the sample. Phase identification is done with cross-correlation and statistical matching of experimental PED patterns with generated electron diffraction templates of all possible (known) phases.[19] Phase maps generated for CS and 5Cr samples using the PED technique are shown in Figure 6. The phase maps clearly show that the inner layer is predominantly magnetite (Fe_3O_4) and outer layer is iron sulfide (FeS). In the case of 5Cr, small amounts of Cr_2O_3 are also seen in the inner layer. The conclusion from TEM/PED analysis is that there is a thin and continuous magnetite layer being formed on the metal surface when it is exposed to naphthenic acid extracts at 650°F.

In contrast, the scales produced after pretreatment with "HVGO-A" are nearly 10x thicker, so they were analyzed by SEM (A & B in Figure 7). As can be seen in the EDS scan for CS, two distinct layers were formed; an outer sulfide-only layer and an inner mixed sulfide-oxide layer. The 5Cr appears to show two layers, but in this case, the inner layer appears to be a mixed Fe and Cr sulfide.

Cross-section analyses of samples (pretreated with "Acids A") after "TAN 3.5 Challenge" using SEM image and EDS data show that both FeS and Fe_3O_4 layers are retained with little change in thickness during the challenge on both CS and 5Cr steel (Figure 8). On the other hand, after "TAN 3.5 Challenge," the CS and 5Cr samples pretreated with "HVGO-A" behave differently (C & D in Figure 7). In the case of CS, the thickness of the FeS layer is thinned from ~8 µm to ~4µm, with some oxide remaining close to the base metal surface. On the other hand, the challenge had little effect on the scale thickness for the 5Cr steel.

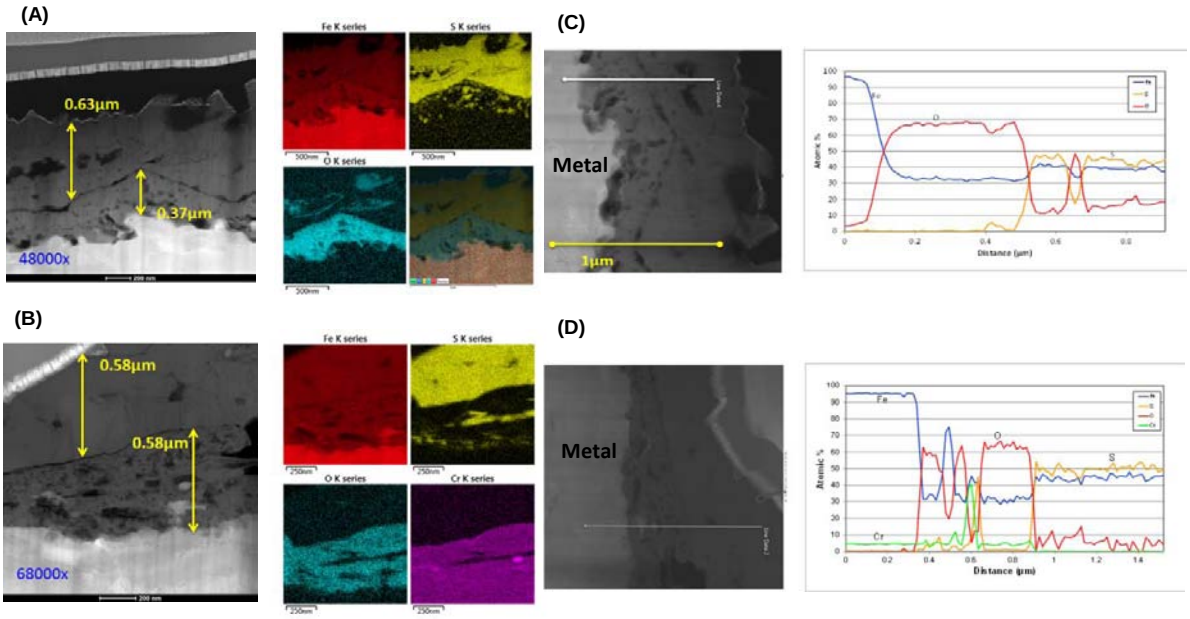

Figure 5: Cross-sectional TEM images and elemental analysis of samples pretreated with "Acids A" (NAP acid extract in white oil) (A) EDS mapping of carbon steel (B) EDS mapping of 5Cr steel (C) EDS line scan for carbon steel, and (D) EDS line scan for 5Cr steel.

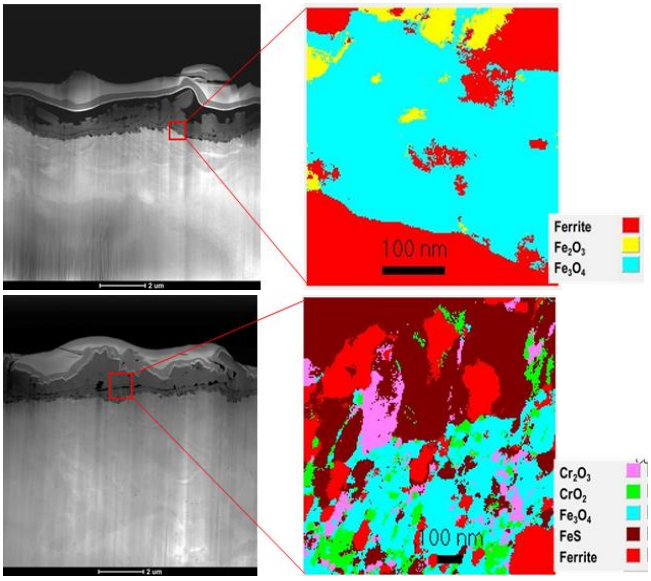

Figure 6: Low magnification cross-sectional TEM images and phase maps (marked area) generated by PED for (a) CS, and (b) 5Cr steel samples pretreated with "Acids A."

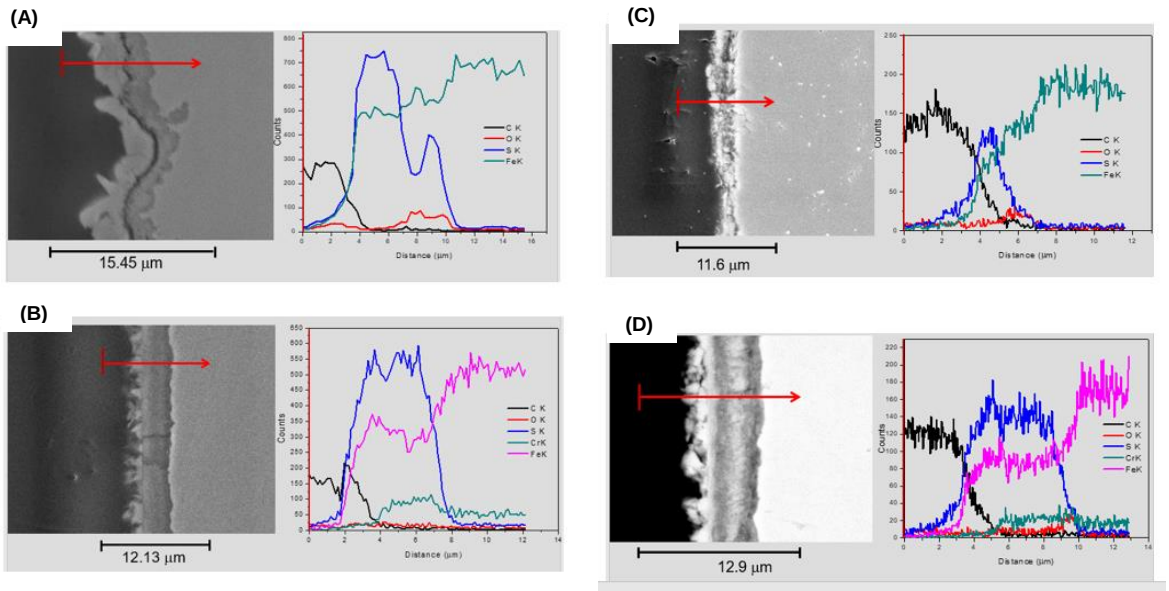

Figure 7: SEM cross-section view and EDS line scan of samples (A) CS pretreated with "HVGO-A" (B) 5Cr steel pretreated with "HVGO-A" (C) CS pretreated with HVGO-A and challenged with "TAN 3.5 Challenge" solution (D) 5Cr steel pretreated with HVGO-A and challenged with "TAN 3.5 Challenge" solution.

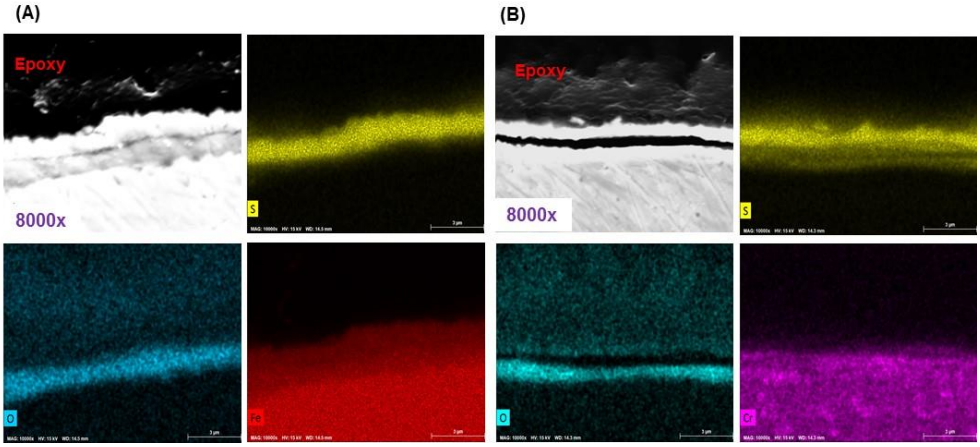

Figure 8: EDS maps of samples pretreated with "Acids A" (NAP acid extract) in autoclave and then challenged with TAN 3.5 solution in HVR; (A) carbon steel (B) 5Cr steel.

HVGO-B vs. Acids B (NAP Acids Extracted from HVGO-B in Mineral Oil)

A similar comparison of HVGO and isolated acid was initiated for "HVGO-B" because it exhibits different behavior in the ICMT "pretreatment-challenge" protocol. In particular, after pretreatment with HVGO-B, both metals were less resistant to acid corrosion than for untreated base metals (Figure 9). Pretreatment in the autoclave with "Acids B" indicate that they are ~8 times less corrosive than "HVGO-B" on both metals. This reduction in corrosivity is more than the ~2 to 3-fold lower value for "Acids A versus HVGO-A." The differences between "Acids A" and "Acids B" can be attributed to the high S/TAN ratio for the latter. Although the S concentration of the isolated acids is similar to their source HVGO, when the "isolated acids" are diluted back to the original TAN in white oils, the "test oils" are depleted of sulfur compounds. The difference between corrosion rates suggest that NAP acids are more dominant in SNAP corrosion with HVGO-A than in HVGO-B, where the sulfur species are more prevalent.

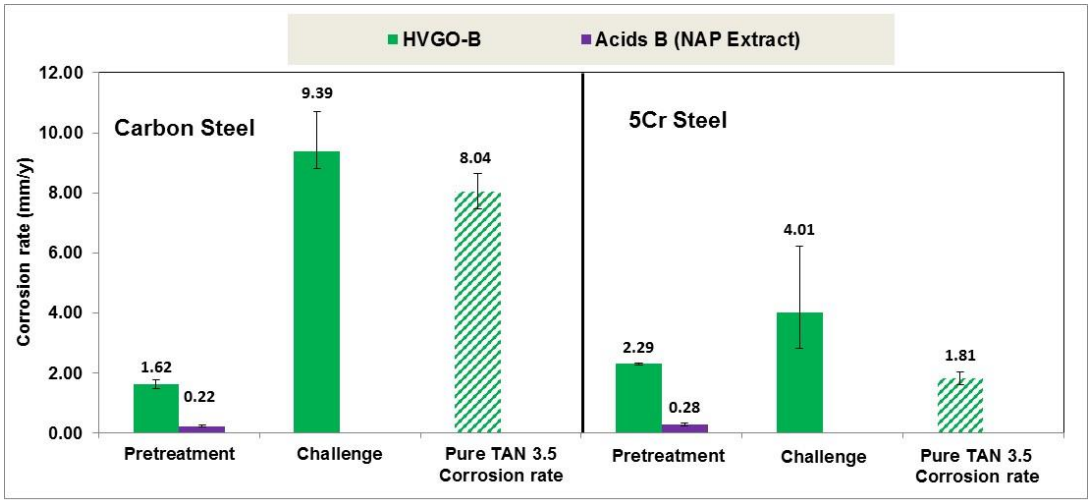

Figure 9: Corrosion rates of carbon steel and 5Cr steel samples pretreated with 'HVGO-B' and its NAP extract ('Acids B').

Pretreatment with "HVGO-B" yields two thick corrosion product layers (Figure 10). On CS, the scale is ~70µm thick with an outer scale consisting of Fe and S, while the thinner inner layer (~6µm) is a mixture

of Fe, S, and O. The corresponding 5Cr steel scale appears to be ~42µm thick with an "eruption" of scale on the surface. The EDS across the eruption appears to show some Cr and O imbedded in an outer scale of FeS, while the ~6 µm inner scale appears to consist mainly of Fe and S with Cr and O enrichment close to the metal interface.

Two layers are also seen in the SEM/EDS cross-sections for samples after pretreatment with "Acids B" (Figure 11). However, these layers are much thinner (of the order of 2µm or less) and EDS elemental analysis show that they are not as distinct as those for pretreatment with "Acids-A." Although the outer layer appears enriched in S relative to O, and *vice versa* for the inner layer, S and O appear to be in both layers. The difference between "Acids B" and "HVGO-B" scale thickness is consistent with the higher S/TAN ratio for HVGO-B.

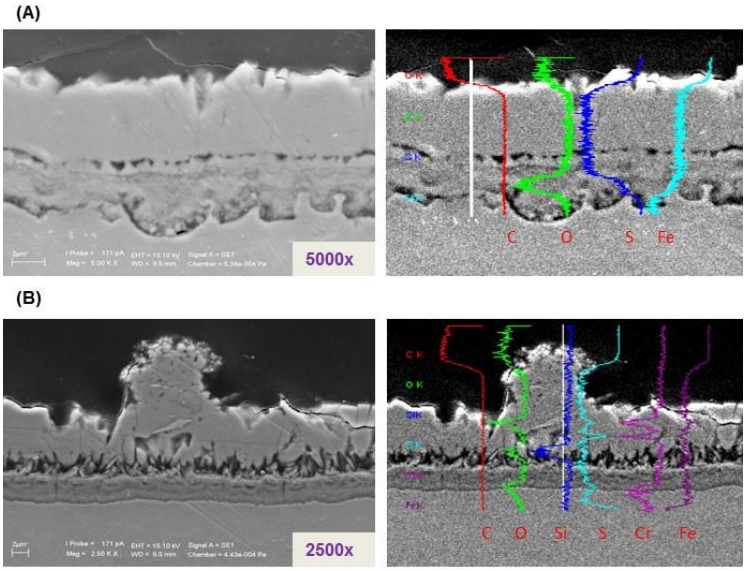

Figure 10: SEM cross-section view and EDS line scan for samples after pretreatment with "HVGO-B"; a) Carbon Steel, b) 5Cr steel.

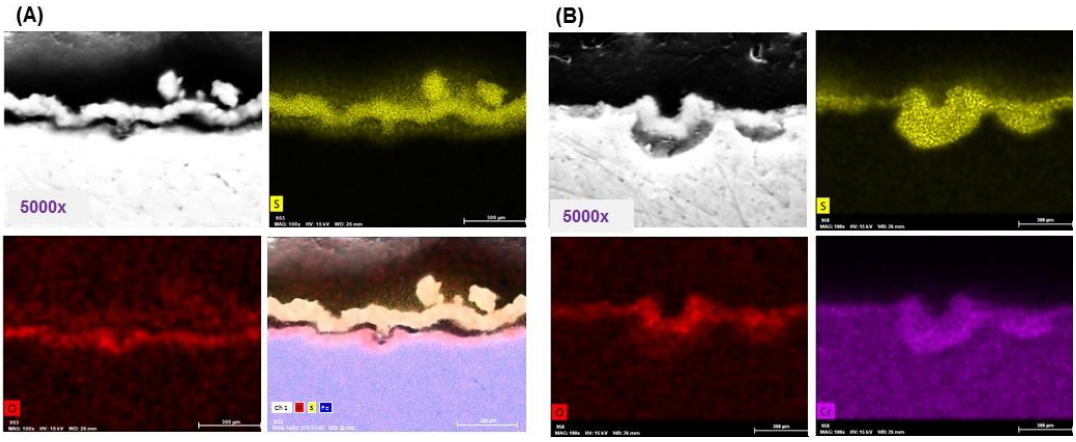

Figure 11: EDS maps of samples pretreated with "Acids B" (NAP extract in mineral oil – TAN 4.43 & S (wt. %): 0.15) in autoclave (A) Carbon steel (B) 5Cr steel.

DISCUSSION

Thin oxide scales, identified as magnetite, have recently been reported under thicker sulfide scales on inner surfaces of refinery pipes and on test samples in stirred autoclave experiments investigating SNAP corrosion.[13,20,21] Oxygen had been detected previously in lab and field samples of corrosion product scales, but its presence was dismissed as experimental artefact.[22] However, a thin, compact magnetite layer close to the metal scale interface has been proposed to be responsible for resistance to further corrosion.[20,21] Model carboxylic acids have been shown to form iron oxide (magnetite) in SNAP corrosion studies. The magnetite is hypothesized to arise from decomposition of iron naphthenates to ketones (R_2(C=O)) and wuztite according to equations (7) & (8).[6,13,21]

$$Fe(RCOO)_2 \rightarrow FeO + CO_2 + RCOR \quad (7)$$

$$4FeO \rightarrow Fe_3O_4 + Fe \quad (8)$$

This hypothesis has been tested and confirmed by model compound tests where a layer of magnetite was formed from model acids in autoclave tests in the absence of reactive sulfur compounds.[6,14] Furthermore, ketones corresponding to model acids were identified in oils at the end of SNAP tests.[12] However, no oxide layer was detected in similar corrosion tests with the same acids in a flow-through reactor unless tested in combination with model sulfur compounds.[13] The latter can be suggested to show that the sulfide layer increases the residence time of iron naphthenates on the scale surface, long enough for their thermal decomposition to magnetite and ketones. Thus, magnetite and ketones are postulated to form from thermal decomposition of iron naphthenates in solution during autoclave testing and under sulfide scale. Similarly, a S/TAN dependence could be inferred from results of SNAP testing of a variety HVGOs by the ICMT pretreatment/challenge protocol.[18] However, model acids are unrepresentative of NAP acids in HVGO; TEM analyses show differences between model acid and HGVO scales.[14] This is particularly evident in the distribution of S and O in the corrosion product scales.

HVGO-A (TAN 5.93/%S 0.87) and HVGO-B (TAN 4.43/ %S 3.65) represent different S/TAN ratios within a group of high TAN HVGOs. Both exhibit pretreatment corrosion rates lower than the S-free TAN 3.5 acids in mineral oil. Although this is consistent with the “common wisdom” that S reduces NAP acid corrosion rates, the higher corrosion rate for HVGO-B (sulfur rich) is contradictory. Furthermore, HVGO-A pretreatment increases resistance to the “TAN 3.5 challenge”, while HVGO-B pretreatment sensitizes the metals so that the challenge corrosion rates increase. On the other hand, the “NAP acids isolated” from both HVGOs, with >20x lower S concentrations, show lower corrosion rates and the formation of oxide-rich inner layers. After pretreatment with “Acids-A,” samples appear to be completely resistant to the TAN 3.5 challenge solution. The cross-section SEM data for the HVGO pretreatments suggest that thicker and less robust scales are formed in pretreatment while the oxygen layer is dependent on the S/TAN molar ratio. At the higher S/TAN ratio, the “HVGO-A” scale is less robust in the challenge than that of “Acids A.” It is proposed that S/TAN molar ratio reflects the difference in the morphology of corrosion scales and concentration of magnetite in the inner layer. Similar effects would be expected for “HVGO-B” and “Acids B” in the challenge environments that are currently under investigation.

CONCLUSIONS

- Solid phase extraction (SPE) methods using APS can be successfully applied for bulk extraction of NAP acids from HVGOs with yields of > 85%.
- Comparison of corrosion by “HVGO” and “NAP acids isolated from them” helps to decouple sulfidation/NAP acid corrosion.
- HVGO containing sulfur and NAP acid species form two distinct corrosion layers (inner Fe_3O_4 layer and outer FeS layer).
- Relative thickness/morphology/composition of the layers depends on the S/TAN molar concentration in the test fluid.

- NAP acids play a critical role in forming iron oxides that decelerate naphthenic acid corrosion.

ACKNOWLEDGEMENTS

This work was supported by Naphthenic Acid Corrosion Joint Industry Project (NAPJIP-II) at the Institute for Corrosion and Multiphase Technology (ICMT), Ohio University. The authors would like to thank all the NAPJIP-II sponsors for their financial assistance and continued support. A special mention to Dr. Danqi Wang of Case Western Reserve University for his assistance with TEM-PED analysis. Also, technical assistance from all the ICMT's lab staff is highly appreciated.

REFERENCES

1. S. D. Kapusta, A. Ooms, A. Smith, W.C. Fort, "Safe Processing of High Acid Crudes", CORROSION 2004, paper no. 04637 (New Orleans, LA: NACE, 2004).

2. Y. Yoon, I. Kosacki, S. Srinivasan, "Naphthenic Acid and Sulfur Containing Crude Oil Corrosion: A Comparative Review", CORROSION 2016, paper no. 7598 (Vancouver, BC: NACE, 2016)

3. A. Turnbull, E. Slavcheva, B. Shone, "Factors controlling naphthenic acid corrosion", CORROSION, 54(11), pp. 922-930, Nov. 1998.

4. Q. Xin, H.D. Dettman, "Corrosivity Study of Sulfur Compounds and Naphthenic Acids under Refinery Conditions", CORROSION 2016, paper no. 7392 (Vancouver, BC: NACE, 2016).

5. E. Slavcheva, B. Shone, A. Turnbull, "Review of naphthenic acid corrosion in oil refining", British Corrosion Journal, *34(*2), pp. 125-131, Feb. 1999.

6. P. Jin, H.A. Wolf, S. Nesic, "Analysis of Corrosion Scales Formed on Steel at High Temperatures in Hydrocarbons Containing Model Naphthenic Acids and Sulfur Compounds", CORROSION 2014, paper no. 4075 (San Antonio, TX: NACE, 2014).

7. G.M. Bota, D.M. Qu, S. Nesic, H.A. Wolf, "Naphthenic acid corrosion of mild steel in the presence of sulfide scales formed in crude oil fractions at high temperature", CORROSION 2010, paper no. 10353 (San Antonio, TX: NACE, 2010)

8. D. Dettman, N. Li, D. Wickramasinghe, Z. Xu, X.N. Chen, G.R. Elliott, J. Luo, "The Influence of naphthenic acid and sulfur compound structure on global crude corrosivity under vacuum distillation conditions", CORROSION 2012, paper no. 1326 (Salt Lake City, UT: NACE, 2012).

9. D.M. Jones, J.S. Watson, W. Meredith, M. Chen, B. Bennett, "Determination of naphthenic acids in crude oils using non-aqueous ion exchange solid-phase extraction", Analytical Chemistry, 73(3), pp. 703-707, Feb. 2001.

10. C.S. Hsu, G.J. Dechert, W.K. Robbins, E.K. Fukuda, "Naphthenic acids in crude oils characterized by mass spectrometry", Energy & Fuels, 14(1), pp. 217-223, Jan. 2000.

11. N.A. Tomczyk, R.E. Winans, J.H. Shinn, R.C. Robinson, "On the nature and origin of acidic species in petroleum. 1. Detailed acid type distribution in a California crude oil", Energy & Fuels, 15(6), pp. 1498-1504, Nov. 2001.

12. P. Jin, W.K. Robbins, G.M. Bota, "Mechanism of magnetite formation in high temperature corrosion by model naphthenic acids", Corrosion Science, 111, pp. 822-834, Oct. 2016.

13. P. Jin, S. Nesic, "Mechanism of magnetite formation in high temperature naphthenic acid corrosion by crude oil fractions", Corrosion Science, 115, pp. 93-105, Feb. 2017.

14. P. Jin, W.K. Robbins, G.M. Bota, "Effect of temperature on scale formation in high-temperature corrosion by model naphthenic acids and sulfur compounds under replenishing conditions", Energy & Fuels, 31(9), pp. 10222-10232, Jul. 2017.

15. S.M. Rowland, W.K. Robbins, Y.E. Corilo, A.G. Marshall, R.P. Rodgers, “Solid-phase extraction fractionation to extend the characterization of naphthenic acids in crude oil by electrospray ionization Fourier transform ion cyclotron resonance mass spectrometry”, Energy & Fuels, 28(8), pp. 5043-5048, Aug. 2014.

16. ASTM D664, “Standard test method for acid number of petroleum products by potentiometric titration”, ASTM International, West Conshohocken, PA, 2005, www.astm.org.

17. C. Xinheng, T. Songbai, “Review and comprehensive analysis of composition and origin of high acidity crude oils”, China Petroleum Processing and Petrochemical Technology, 13(1), pp. 6-15, Mar 2011.

18. G.M. Bota, S. Nesic, “Naphthenic acid challenges to iron sulfide scales generated in-situ from model oils on mild steel at high temperature”, CORROSION 2013, paper no. 2512 (Orlando, FL: NACE, 2013).

19. D. Viladot, M. Veron, M. Gemmi, F. Peiro, J. Portillo, S. Estrade, J. Mendoza, N. Llorca-Isern, S. Nicolopoulos, “Orientation and phase mapping in the transmission electron microscope using precession-assisted diffraction spot recognition: state-of-the-art results”, Journal of Microscopy, 252(1), pp. 23-34, Oct. 2013.

20. M.M. Barney, B. Embaid, A. Nissan, “Identifying phases in protective scale formed during high temperature corrosion”, Corrosion Science, 127, pp. 21-26, Oct. 2017.

21. H.A. Wolf, F. Cao, S.C. Blum, A.M. Schilowitz, S. Ling, J.E. Mclaughlin, S. Nesic, P. Jin, G.M. Bota, “Method for identifying layers providing corrosion protection in crude oil fractions”, U.S. patent no. 9,140,640, Sep. 2015.

22. B.S. Huang, W.F. Yin, D.H. Sang, Z.Y. Jiang, “Synergy effect of naphthenic acid corrosion and sulfur corrosion in crude oil distillation unit”, Applied Surface Science, 259, pp. 664-670, Oct. 2012.